Available online at www.sciencedirect.com
SCIENCE DIRECT®
European Journal of Mechanics B/Fluids 24 (2005) 314–327

The evolution of freely-decaying, isotropic, two-dimensional turbulence

A.J. Lowe, P.A. Davidson *

Department of Engineering, University of Cambridge, UK

Received 23 September 2003; received in revised form 9 March 2004; accepted 16 September 2004

Available online 6 November 2004

Abstract

This paper discusses the decay of freely-evolving, two-dimensional turbulence. We present numerical simulations in which particular care is taken to avoid unphysical pollution from periodic boundary conditions. Batchelor's classical theory, which assumes that the kinetic energy is the only invariant of the flow, predicts that the integral scale grows as $l \sim t$. In line with the results of Herring et al. [Evolution of Decaying Two-dimensional Turbulence and Self-similarity, Trends in Mathematics, Birkhäuser Verlag Basel, Switzerland, 1999], and many others, our DNS results show that l grows approximately as $t^{1/2}$. Bartello and Warn [J. Fluids Mech. 326 (1996) 357–372], and McWilliams [J. Fluids Mech. 146 (1984) 21–43], suggested that, in the limit $\mathrm{Re} \to \infty$, two-dimensional turbulence possesses a second invariant: the peak in vorticity. It is now widely accepted that this explains the failure of Batchelor's theory. However, as yet, there is no satisfactory explanation for the $t^{1/2}$ growth in l.

Periodic boundary conditions impose mirror image long-range correlations of velocity and vorticity. Lilly [J. Fluid Mech. 45 (2) (1971) 395–415], and Davidson [Turbulence: An Introduction for Scientists and Engineers, Oxford University Press, 2004], note that these correlations have the potential to influence the dynamical behavior of the turbulence. Varying the energy-containing length-scale of the turbulence relative to the size of the periodic domain allows this effect to be investigated. To this end, we introduce the box-ratio, $l_{\mathrm{domain}}/l_{\mathrm{turbulence}}$, as a measure of the number of energy containing eddies in our simulations. Over a wide range of box-ratios we show that l grows approximately as $t^{1/2}$, the enstrophy decays as $\sim t^{-1}$ (at least for large Re), and the l-normalised vorticity correlations more or less collapse onto a single, self-similar curve. We provide one possible explanation for the observed $t^{1/2}$ growth of l.

1. Introduction

1.1. The problem

We are interested in freely-decaying, homogeneous, two-dimensional turbulence at high Reynolds number. In 1969 Batchelor, [1], proposed a model of such turbulence in which there is a self-similar decay of the energy spectrum, a linear growth in the integral length-scale, $l \sim t$, and a quadratic decay of enstrophy, $\omega^2 \sim t^{-2}$. No simulation of freely-decaying isotropic turbulence has found a t^{-2} decay in enstrophy, or a linear growth in l. For example, the large Re simulations of Chasnov, [2], Clercx and Nielsen, [3], and Ossia and Lesieur, [4], suggest the enstrophy decays as $\sim t^{-0.8}, t^{-1.0}$ and $t^{-1.1}$, respectively,

* Corresponding author.
E-mail address: pad3@eng.cam.ac.uk (P.A. Davidson).

0997-7546/$ – see front matter
doi:10.1016/j.euromechflu.2004.09.003

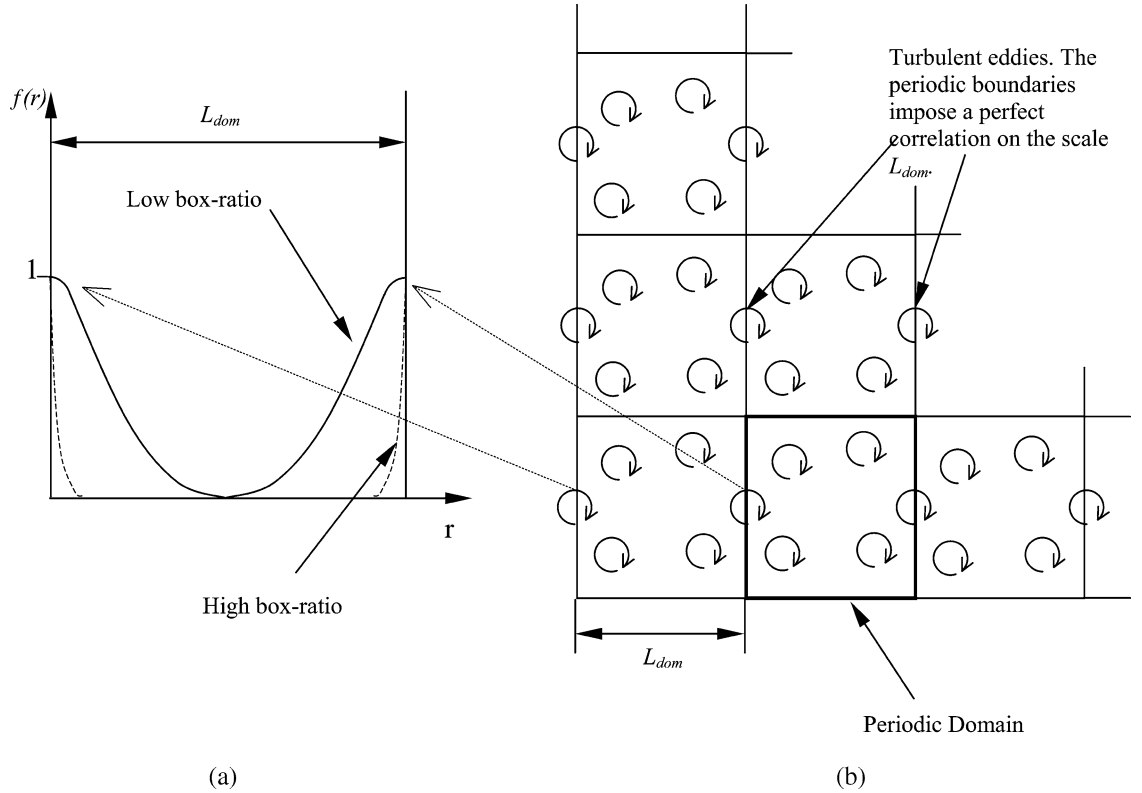

Fig. 1. The schematic representation of periodic boundary conditions supporting the mirror image long-range velocity correlations. (a) The shape of the longitudinal correlation function, $f(r)$; (b) flow in a periodic domain and it's neighbours.

while those of Herring et al., [5], and Clercx and Nielsen, [3], suggest $l \sim t^{0.5}$ and $l \sim t^{0.45}$, respectively. However, Batchelor's theory is based on the existence of only one invariant: the kinetic energy. Observations and analysis of Bartello and Warn, [6], and McWilliams, [7], suggest that, for $\mathrm{Re} \to \infty$, two-dimensional turbulence also remembers the peak value of vorticity, a view which is given support by the analyses of Legras, Dritschel others. (See, for example, [8,9].) We bring these results together and use DNS to investigate the evolution of the enstrophy, ω^2, and the integral length-scale, l, defined as,

$$l = (2\overline{u^2}/\overline{\omega^2})^{1/2}, \quad u^2 = \overline{u_x^2} = \overline{u_y^2}. \tag{1}$$

(Here the overbar represents a spatial average.)

Direct Numerical Simulation (DNS) of freely-decaying turbulence is often undertaken in a periodic domain and this is the approach adopted here. However, the periodic boundary conditions impose unphysical long-range correlations on the scale of the box and these have the potential to influence the dynamical behaviour of the turbulence (Lilly, [10], Davidson, [11]). This is illustrated in Fig. 1.

In order to measure the relative size of the computational domain we introduce the box-ratio, defined as,

$$B = l_{\mathrm{dom}}/l. \tag{2}$$

Here l_{dom} is the characteristic size of the domain (in our simulations the length of one side of the square computational domain) and l is the integral scale of the turbulence determined from (1). The box-ratio is crucial in numerical experiments. If the box-ratio is too small the periodic boundary conditions can influence the dynamics within the square in an unphysical way. A sensitive test of the influence of periodicity is the low wave-number, k^3, region of the energy spectrum, $E = C(t)k^3$. That is, if B is too small anomalous results can be obtained for the evolution of $C(t)$. Batchelor's self-similar theory predicts $C \sim t^4$, whereas, Ossia, [4], did not find a t^4 growth of $C(t)$. We shall investigate the behaviour of $C(t)$, l and ω^2 over a range of box-ratios for mature,[1] two-dimensional, freely-decaying, isotropic turbulence.

[1] We use the word 'mature' to indicate a state in which the precise details of the initial conditions have been largely erased and non-linearity has had sufficient time to distribute energy over the full range of length-scales.

1.2. The failure of Batchelor's classical theory of two-dimensional turbulence

Over the past thirty years, Batchelor's paper on the self-similar decay of homogeneous turbulence has generated considerable interest and has been referenced extensively. Although now known to be flawed, it is useful to review this work, if only to put the subsequent analysis into context. Batchelor considers the evolution of the kinetic energy per unit mass,

$$\frac{1}{2}\mathbf{u}^2, \quad \mathbf{u} = (u_x, u_y, 0), \tag{3}$$

and enstrophy,

$$\overline{\omega^2}, \quad \boldsymbol{\omega} = (0, 0, \omega). \tag{4}$$

No vortex stretching occurs in two-dimensional turbulence and so the enstrophy decays as,

$$\frac{1}{2}\frac{\mathrm{d}\overline{\omega^2}}{\mathrm{d}t} = -\upsilon\overline{(\nabla\omega)^2}. \tag{5}$$

Thus the enstrophy is bounded from above by its initial value. This has implications for the decay of kinetic energy. In freely-decaying, homogeneous turbulence, the decay of kinetic energy is governed by,

$$\frac{1}{2}\frac{\mathrm{d}\overline{\mathbf{u}^2}}{\mathrm{d}t} = -\upsilon\overline{\omega^2}. \tag{6}$$

However, we know that $\overline{\omega^2}$ is bounded above by its initial value and so for high Reynolds number, i.e. $\upsilon \to 0$, kinetic energy is approximately conserved for any finite period of time:

$$\frac{1}{2}\overline{\mathbf{u}^2} = u^2 = \text{constant}. \tag{7}$$

Consequently, Batchelor [1] proposed that for high Reynolds number, fully-developed, homogeneous, two-dimensional turbulence, the only quantity the turbulence remembers is the kinetic energy. Thus, the parameters governing the energy spectrum, $E(k)$, are the velocity scale, u, wave number, k, viscosity, υ, and time, t. However, outside the viscous dissipation range viscosity is not a relevant parameter and so in this region $E = E(k, u, t)$. The only dimensionally consistent possibility for the energy spectrum is then,

$$E(k) \sim u^3 t\, D(kut), \tag{8}$$

where D is a dimensionless function and u is invariant. It follows that the integral-scale, l, should grow as,

$$l \sim ut. \tag{9}$$

Since $E \sim k^3$ for small k (Davidson [11, §10.1.6]), Batchelor's theory implies that the low-wave number part of the energy spectrum should evolve as,

$$E(k) \sim u^6 t^4 k^3. \tag{10}$$

A limited amount of numerical data is available for the low-wave number region of $E(k)$. Ossia, [4], and Chasnov, [2], both required ensemble averaged results to determine the form of the entire energy spectrum. Neither the results of Ossia nor Chasnov show a t^4 growth in the k^3, low-wave number region. This is just one of many indications that Batchelor's theory is incomplete. A second important consequence of Batchelor's self-similar theory relates to the enstrophy,

$$\overline{\omega^2} = 2\int k^2 E(k)\,\mathrm{d}k. \tag{11}$$

This is predicted to decay as,

$$\overline{\omega^2} \sim W t^{-2}, \quad W = 2\int z^2 D(z)\,\mathrm{d}z. \tag{12}$$

As we noted in Section 1.1, the large Re results of Chasnov [2], Clercx and Nielsen [3], and Ossia and Lesieur [4] suggest an enstrophy decay of $\sim t^{-0.8}$, $t^{-1.0}$ and $t^{-1.1}$, respectively. Again we see that Batchelor's theory is at odds with the observations.

There are two final consequences of Batchelor's theory. First, following Kraichnan, [12], Batchelor reformulated Kolmogorov's equilibrium theory, [13], applied to the enstrophy, and concluded that the form of the energy spectrum in the inertial

range should be k^{-3}. (See Kraichnan and Montgomery, [14], for a review.) Second, following the procedure of Batchelor [15, §3.1], the behaviour of the energy spectrum in the neighbourhood of $k = 0$ is of the form (Davidson [11, §10.1.6]),

$$E(k) = C(t)k^3 + \mathrm{O}(k^5) = \frac{1}{4} I_{2\mathrm{D}} k^3 + \mathrm{O}(k^5), \quad I_{2\mathrm{D}} = u^2 \int_0^\infty r^3 f(r)\,\mathrm{d}r. \tag{13}$$

Here $I_{2\mathrm{D}}$ to the two-dimensional version of Loitsyansky's integral. As in three-dimensions, an evolution equation for Loitsyansky's integral may be obtained from the Karman–Howarth equation. It is (Davidson [11]),

$$\mathrm{d}I_{2\mathrm{D}}/\mathrm{d}t = \lfloor u^3 r^3 K \rfloor_{r\to\infty}, \tag{14}$$

where $K(r)$ is the longitudinal triple correlation function. Batchelor's self-similar theory predicts that K is a function of r/ut only, and since u^2 is the only invariant of the theory, K must fall of as r^{-3} for large r. It follows from (14) that $I_{2\mathrm{D}} \sim C(t) \sim u^6 t^4$, which is consistent with (10). As noted above, this t^4 behaviour is not observed in the simulations.

1.3. Refining the classical view

Bartello and Warn, [6], have suggested that Batchelor's theory may be refined by introducing a second invariant. The argument goes like this. At modest values of Re neither u^2 nor the peak vorticity, $\hat{\omega}$, are conserved [3]. However, at high Re $\hat{\omega}$ tends to be located at the centre of coherent vortices, and these robust structures shelter their interior vorticity from the external strain field in line with the Weiss criterion (McWilliams [7]). Thus $\hat{\omega}$ declines due to diffusion only. However, this is a small effect at large Re, and so we expect $\hat{\omega}$ to be conserved in the limit $\mathrm{Re} \to \infty$ [8,9]. Let us, therefor, suppose that the turbulence remembers both u^2 and the peak vorticity, $\hat{\omega}$. Then dimensional analysis tells us that, for large Re, (8) must be replaced by,

$$E(k) \sim u^3 t\, D(kut, \hat{\omega}t). \tag{15}$$

The integral scale defined by (1) then takes the form $l = utF(\hat{\omega}t)$ for some dimensionless function F. The particular case of,

$$D = (\hat{\omega}t)^{-1/2} D^+(kut/\sqrt{\hat{\omega}t}), \tag{16}$$

is of some interest since this yields a self-similar energy spectrum of the form,

$$E(k) = u^2 l^+ D^+(kl^+) \tag{17}$$

where,

$$l^+ \sim ut/\sqrt{\hat{\omega}t} \sim t^{1/2}, \quad \overline{\omega^2} \sim \hat{\omega} t^{-1}, \quad I_{2\mathrm{D}} \sim u^6 t^2/\hat{\omega}^2. \tag{18}$$

We shall see shortly that the $l \sim t^{1/2}$ scaling is indeed observed in our simulations across the range of Reynolds numbers realised. However, because of the modest values of Re used in our simulations we do not have conservation of energy, nor of $\hat{\omega}$. It is difficult, therefore, to verify directly the high-Re scalings (16)–(20). Never-the-less, the robustness of the result $l \sim t^{1/2}$, and the convincing arguments behind (15), suggest that the scalings (16)–(20) should apply when $\mathrm{Re} = ul/\upsilon$ is large and we shall see that this is more or less compatible with the findings of Ossia and Lesieur [4], Herring et al. [5], Chasnov [2] and Clercx and Nielsen [3].

2. Our numerical method

We use the well established pseudospectral collocation method, the origins of which date back to the early 1970's (Orszag and Patterson, [16]) for three-dimensional simulations and Fox and Orszag, [17], for two-dimensional simulations. Our DNS experiments are dealiased using the so-called '2/3 rule', the non-linear terms are calculated in physical space and we use a second-order Runge–Kutta time stepping scheme. The numerical scheme is described in more detail in Lowe, [18], and details of the simulations are tabulated in Appendix A.

The two-dimensional geometry we use is square and the boundary conditions are periodic in both directions. Canuto et al., [19], and the NASA report of Rogallo, [20], describe the pseudospectral technique adopted here. Usually, two-dimensional turbulence simulations use a stream-function-vorticity formulation (examples are Fox and Orszag, [17], Lilly, [10]). However, we have selected the rotational form of the Navier–Stokes equation,

$$\partial \mathbf{u}/\partial t + \boldsymbol{\omega} \wedge \mathbf{u} = -\nabla P + \upsilon \nabla^2 \mathbf{u}, \tag{19}$$

as the basis of our numerical scheme as this allows ease of access to the velocity and vorticity fields during the computations.

3. The DNS results: the evolution of the integral scale and enstrophy

We now turn to the DNS. In this section we discuss the growth of the length-scale, l, defined by (1). We show that the growth in the integral scale, l, is reasonably well predicted by $l \sim t^{1/2}$, in line with the findings of Herring [5], and Clercx and Nielsen [3]. We then consider the evolution of the enstrophy. By assuming the enstrophy decay can be characterised by a power law, we show that the decay exponent is dependent on both the box-ratio and $\mathrm{Re} = ul/\upsilon$. In line with others, we do not find the t^{-2} decay predicted by Batchelor's self-similar theory. Rather, we find that the decay law at large Re is more like t^{-1}, which is consistent with the scalings presented in Section 1.3 and the results of Chasnov [2], Ossia [4], and Clercx and Nielsen [3].

3.1. The integral scale

Fig. 2 shows the evolution of the normalised integral scale, $\langle l/l_0 \rangle$, against eddy turnovers, t/τ_e. (Here τ_e is the initial turnover time, l_0 the initial value of l, and $\langle \sim \rangle$ represents the ensemble of spatial averages from at least 16 different simulations.) We observe that the growth is well represented by $l \sim t^{1/2}$. The results presented in Fig. 2 span the entire duration of the numerical simulations. The highest box-ratio simulations show the evolution from 0 to 34 eddy turnovers. We note that for t less than, say, $10\tau_e$ the history of l could depend on the initial conditions. However, once the turbulence is mature, the $l \sim t^{1/2}$ scaling works reasonably well.

The effect of box ratio and $\mathrm{Re} = ul_0/\upsilon$ on the exponent n in the power law $l \sim t^n$ is shown in Table 1. The exponents are obtained by fitting a power law to the data for $t > 10\tau_e$. Although there is some scatter in the exponents, they all lie close to 0.5, with a mean value over all the simulations of 0.52. Note that, although ensemble average statistics are desirable, single realisation simulations using spatial averages yield reasonable and repeatable results for the growth of l and the decay of enstrophy.

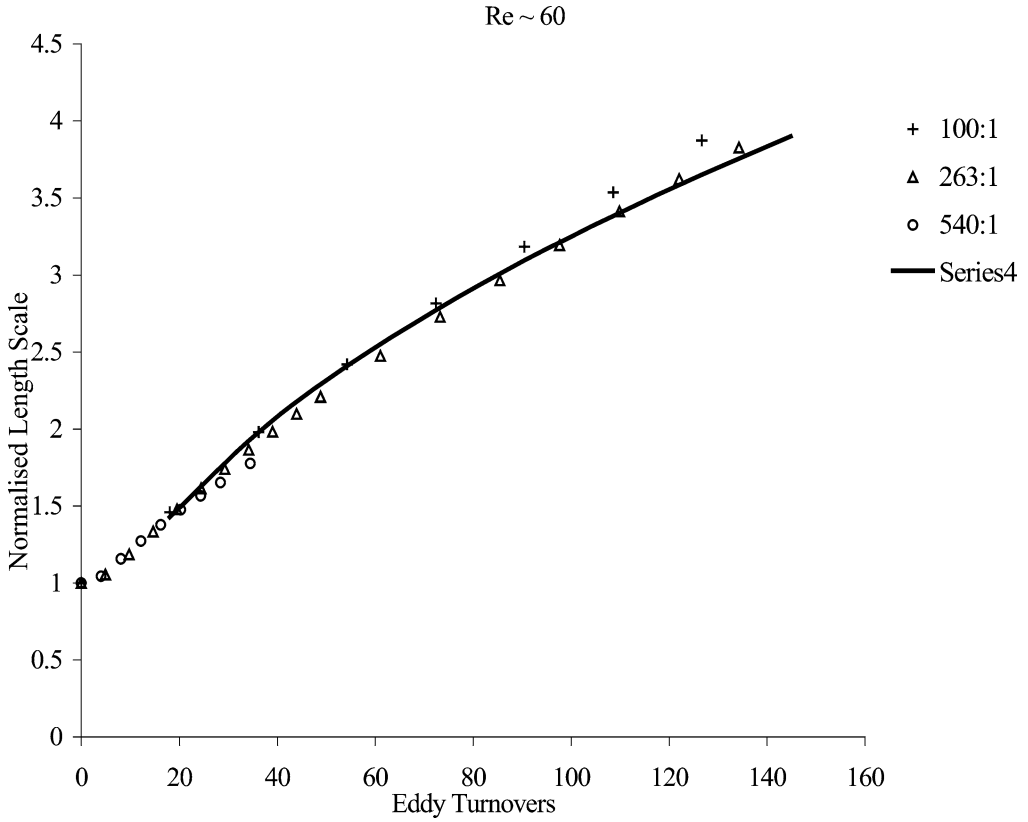

Fig. 2. The evolution of the normalised integral scale $\langle l/l_0 \rangle$, against eddy turnovers (t/τ_e) for $\mathrm{Re} = ul_0/\upsilon = 60$ and box-ratios of 100 : 1, 263 : 1 and 540 : 1. The solid line is a fit of the form $(a + b(t/\tau_e))^{1/2}$, $b = 0.104$.

Table 1
The value of n, the best-fit exponent to the power-law $l \sim t^n$ ($\langle\sim\rangle$ indicates ensemble averaged results)

Re	Box-ratio				
	32	50	69	100	263
∼60	0.52	0.51	0.55	⟨0.53⟩	⟨0.56⟩
∼120	0.52	0.51	0.53	⟨0.50⟩	
∼240	⟨0.52⟩	0.49	⟨0.51⟩		

Table 2
The value of γ, the time-averaged enstrophy decay exponent for various box-ratios and Re. $\langle\sim\rangle$ indicates ensemble averaged results

Re	Box-ratio				
	32	50	69	100	263
∼60	1.29	1.27	1.33	⟨1.37⟩	⟨1.45⟩
∼120	1.17	1.22	1.26	⟨1.19⟩	
∼240	⟨1.12⟩	1.12	⟨1.12⟩		

Table 3
The value of α, the time-averaged energy decay exponent for various box-ratios and Re

Re	Box-ratio				
	32	50	69	100	263
∼60	0.26	0.25	0.24	⟨0.32⟩	⟨0.34⟩
∼120	0.14	0.19	0.20	⟨0.20⟩	
∼240	⟨0.08⟩	0.14	⟨0.11⟩		

3.2. Enstrophy

Table 2 lists the time-averaged decay exponent, γ, for the enstrophy for a range of both Re = ul_0/υ and box-ratios. We have determined the time-averaged decay exponent for the mature period of the evolution only. In general, the time taken for the decay exponent to fall onto an asymptotic value is dependent on the form of the initial energy spectrum, but is of the order of $t \sim 10\tau_e$. We immediately observe both an Re and box-ratio dependence for the magnitude of γ.

The exponent γ ranges in magnitude from 1.1 to 1.5. Note that, as Re increases, γ tends towards a value of the order of unity, as suggested by (18). Perhaps the most important point to emphasise here is that the variation of γ with Re is almost entirely due to the non-negligible rate of decay of energy for the range of Reynolds numbers considered here. This can be seen by comparing Table 1 with Table 3, which show the exponents in the power laws $l \sim t^n$ and $u^2 \sim t^{-\alpha}$ respectively. As Re changes α varies considerably, while n remains close to 0.5. Evidently, the $\sqrt{t}$ growth in l is a robust result. Note that, as Re increases, and energy is better conserved, we approach the scalings suggested by (18).

We might note, by way of comparison, that Chasnov, [2], also investigated freely-decaying turbulence using numerical simulations. Chasnov found the asymptotic decay exponents, γ, ranged from ∼1.6 to 0.8 when Re that varied from 32 to 4096. The general trend seen in both our and Chasnov's data is that the enstrophy decay exponent falls in magnitude as Re is increased, reaching a value around unity for large Re. Similar results were obtained by Herring et al. [5], Clercx and Nielsen [3] and Ossia and Lesieur [4].

4. More DNS: vorticity correlations

We now consider the ensemble averaged vorticity correlation, $\langle\omega\omega'\rangle$. This is calculated using the technique described in Lowe [18]. Fig. 3 shows the evolution of the ensemble averaged normalised vorticity correlation over a range of eddy turnovers for Re = $ul_0/\upsilon = 60$. The averages were performed over 48 realisations. The different curves represent the correlations at $t/\tau_e = 0, 9.76, 19.5, 39.5$ and 84.5. The arrow in Fig. 3 indicates the growth in the length-scale of the turbulence.

The form of the initial conditions determines the nature of the vorticity correlation during the initial evolution of the turbulence. In particular, the distance over which the correlation oscillates about the r-axis lengthens when the energy is closely peaked around a narrow range of wave numbers. This type of correlation is found in peaked spectra of the type used by Bartello

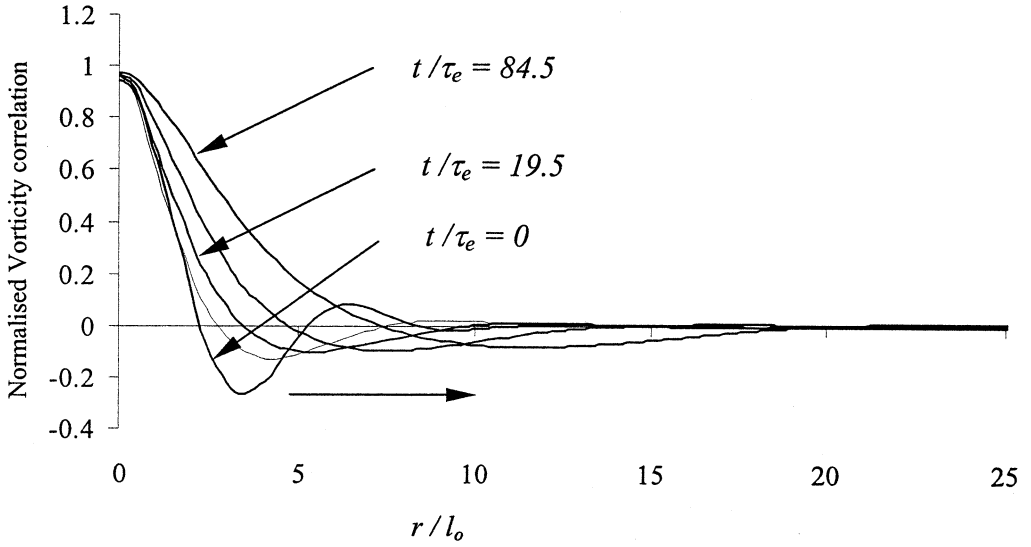

Fig. 3. The ensemble averaged vorticity correlation $\langle \omega \cdot \omega' \rangle / \langle \omega^2 \rangle$ plotted against r normalized by the initial integral scale. The curves correspond to $t = 0, 9.76, 19.5, 39.5$ and 84.5 eddy turnovers. The arrow indicates increasing time. Group B simulations. Re $= 60$, $B = 263 : 1$ and $N = 1024$.

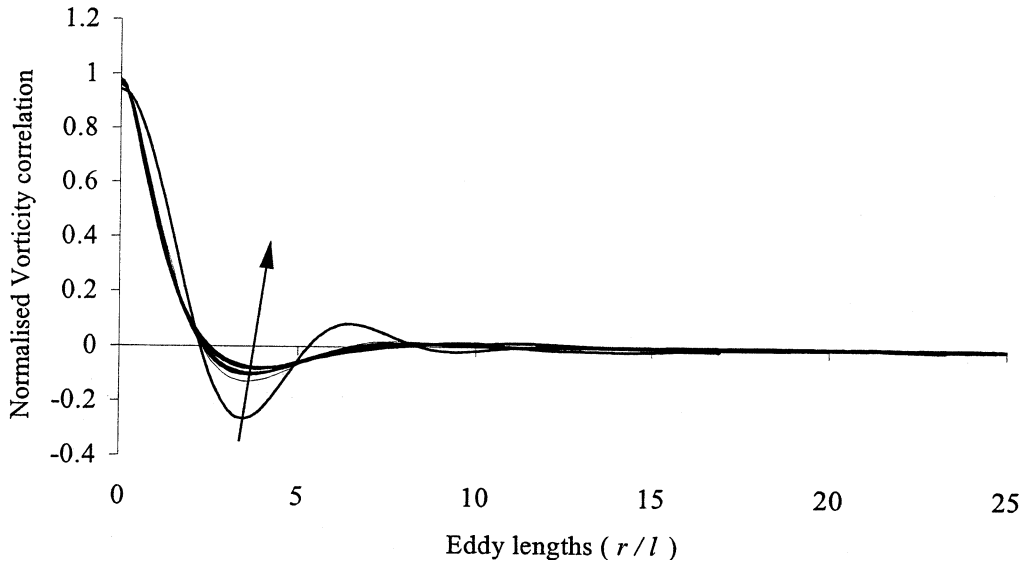

Fig. 4. The ensemble averaged vorticity correlations $\langle \omega \cdot \omega' \rangle / \langle \omega^2 \rangle$ plotted against r normalised by the integral scale l. The curves correspond to $t = 0, 9.76, 19.5, 39.5, 84.5$ and 134 eddy turnovers. The arrow indicates increasing time. Group B simulations.

and Warn, [6]. Here the initial correlations oscillate over $10 \rightarrow 15$ integral scales, as shown above. However, as the turbulence evolves, and the spectrum fills out and matures, the long-range nature of the correlations erodes. We then find correlations similar in form to those shown in Fig. 3 after $\sim$20 eddy turnovers.

Fig. 4, shows the evolution of the vorticity correlation scaled with the calculated integral scale, l. The arrow indicates increasing time and the box-ratio is $263 : 1$. We observe that, for $t > 10\tau_e$, there is a reasonable collapse of the vorticity correlation onto a single curve. However, the collapse is by no means perfect.

Fig. 5 shows the overlay of the two sets of scaled correlations (Groups B and D) for a range of eddy turnovers from $\sim$20 to $\sim$140 eddy turnovers. The correlations show a reasonable collapse of the scaled vorticity correlation onto a single, self-similar curve. The scaled correlations are negligible from r greater than $\sim 7l$. The correlations calculated in simulations Groups A and C are similar to the results presented here.

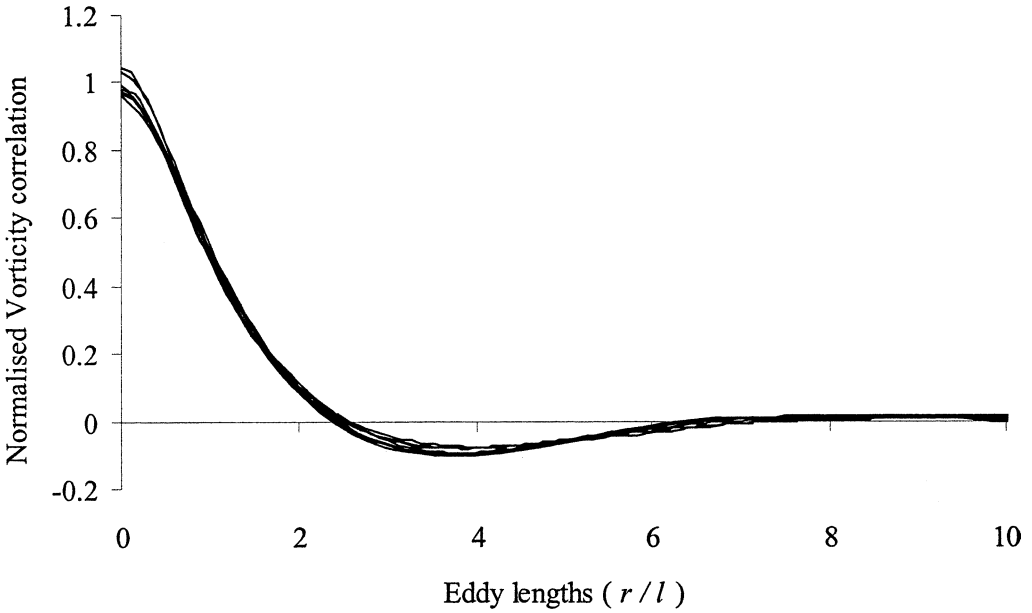

Fig. 5. The ensemble averaged vorticity correlations $\langle \omega \cdot \omega' \rangle / \langle \omega^2 \rangle$ plotted against r normalised by the integral scale. The curves correspond to ∼20 to ∼140 eddy turnovers. Group B (box ratio of 263 : 1) and D (box ratio of 100 : 1) simulations.

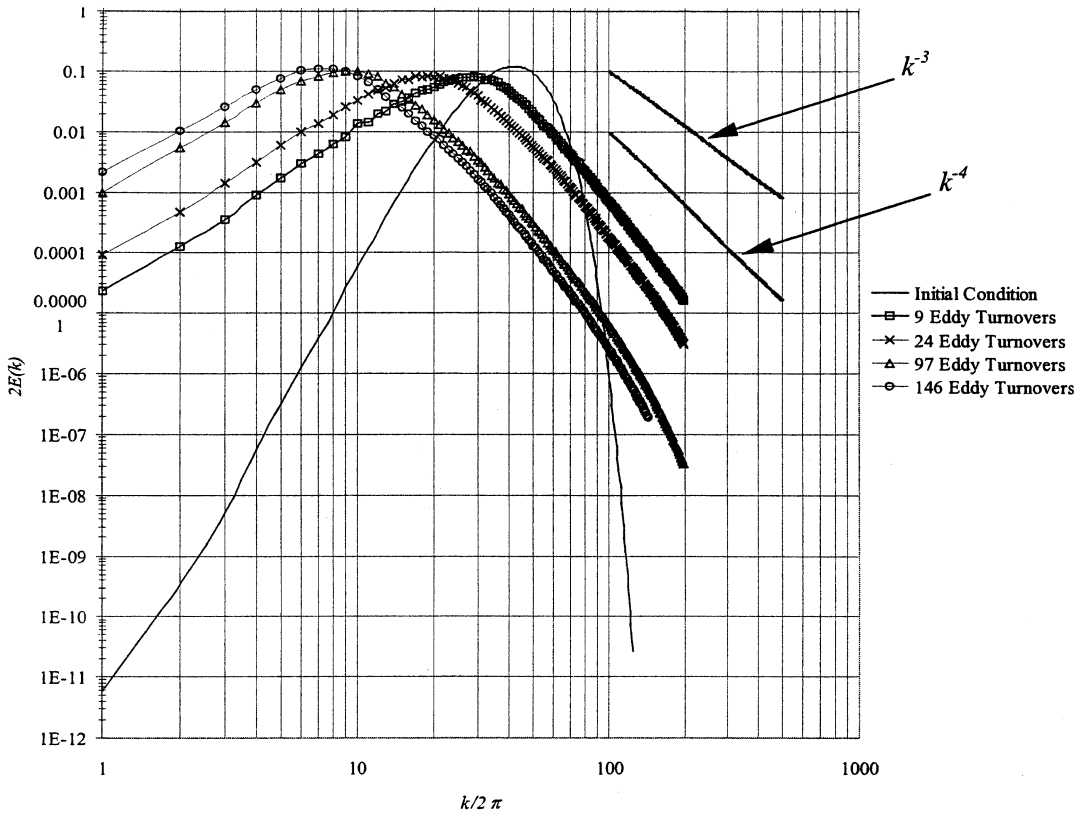

Fig. 6. The log-log plot of ensemble averaged energy spectrum, $E(k)$, against wave number, $k/2\pi$, for $t = 0, 9, 24, 97$ and 134 eddy turnovers. Group B simulations.

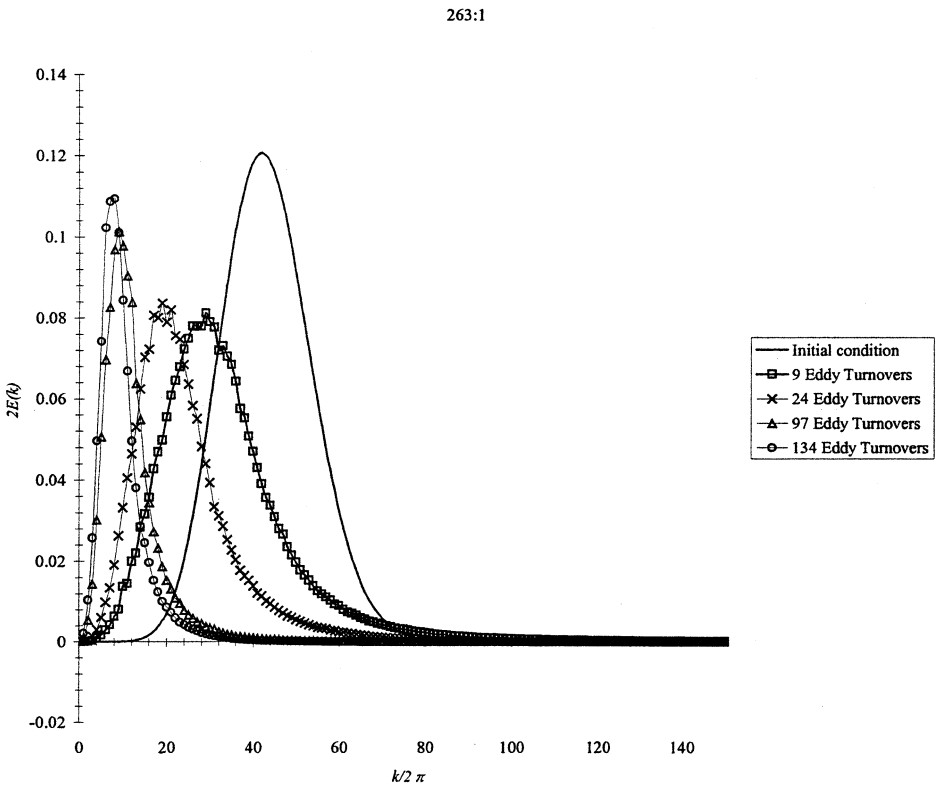

Fig. 7. The linear-linear plot of ensemble averaged energy spectrum, $E(k)$, against wave number, $k/2\pi$, for $t = 09, 24, 97$ and 134 eddy turnovers. Group B simulations.

5. The computed energy spectra

Fig. 6 (log-log) and Fig. 7 (linear-linear), show the evolution of the ensemble averaged energy spectrum, $E(k)$, over a range of eddy turnovers. The results presented are from Group B simulations. The Reynolds number is $\mathrm{Re} = 60$ and the box-ratio is 263 : 1. After ∼10 eddy turnovers a mature spectrum has formed. The low wave number region of the spectrum is approximately k^n, with $n \sim 2.9$. None of the simulations, Groups A–D, show a low wave number region with $n = 3$, indicating a lack of resolution at small k even at a box ratio of 540. The value of Re is too low for an inertial range to form although there exists a range of k in which the spectrum is of the form k^{-m} with m ranging in magnitude from 3 to 4, which is consistent with the results of Chasnov, [2], and Herring et al., [21].

Evidently, the kinetic energy moves to the larger length-scales (smaller k) as the simulations proceed, as we would expect when l increases with time. This means that the problem of resolving the low-k end of the spectrum becomes more pronounced as time increases. This is clearest in Fig. 7. The energy spectrum concentrates around the lower modes and the bulk of the energy does not span a large range of wave numbers. (This is less obvious in the log-log plot.) One implication of this is that it is difficult to obtain reasonable statistics from the lower modes. Chasnov, [2], and Ossia, [4], suggest that in order to obtain reliable statistical information, ensemble statistics are required. However, if the turbulence is influenced by the periodic boundary conditions because l is too close to L_{box}, then no amount of ensemble averaging can remedy this.

Fig. 8 (log-log) and Fig. 9 (linear-linear), show the evolution of the ensemble average enstrophy spectrum, $k^2E(k)$, over a range of eddy turnovers. The Reynolds number is $\mathrm{Re} = 60$, the box-ratio 263 : 1, and the results are from Group B simulations. We did not find a significant range of wave numbers over which the spectrum displayed an inertial enstrophy cascade, k^{-1}, region. This is not surprising in view of the limited value of Re in our simulations. All simulations Groups A–D showed similar results.

Let us now consider the degree to which $E(k, t)$ is self similar. Fig. 10 shows the evolution of the scaled spectrum (E/u^2l) for $\mathrm{Re} = 60$, a box-ratio = 263 : 1 and at $t/\tau_e = 9, 24, 97$ and 134. We observe that the scalings collapse the spectrum reasonably well, with the exception of the low wave number region. (The arrow indicates increasing time.) The failure of self-similar scaling for the small k is in line with the results of Chasnov, [2], Bartello and Warn, [6], and Ossia and Lesieur, [4].

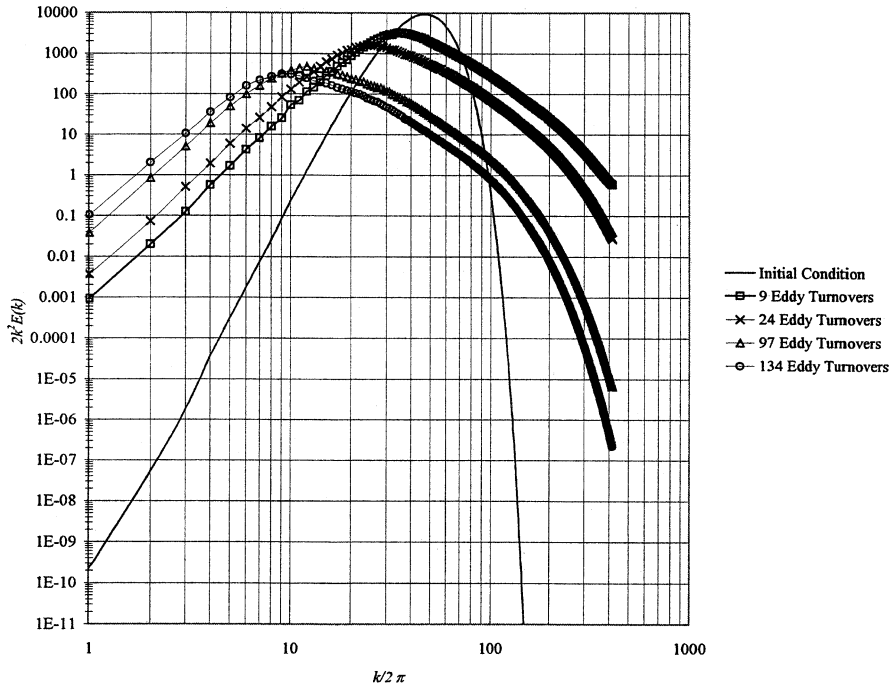

Fig. 8. The log-log plot of ensemble averaged enstrophy spectrum, $k^2E(k)$, plotted against wave number, $k/2\pi$, for $t = 0, 9, 24, 97$ and 134 eddy turnovers. Group B simulations.

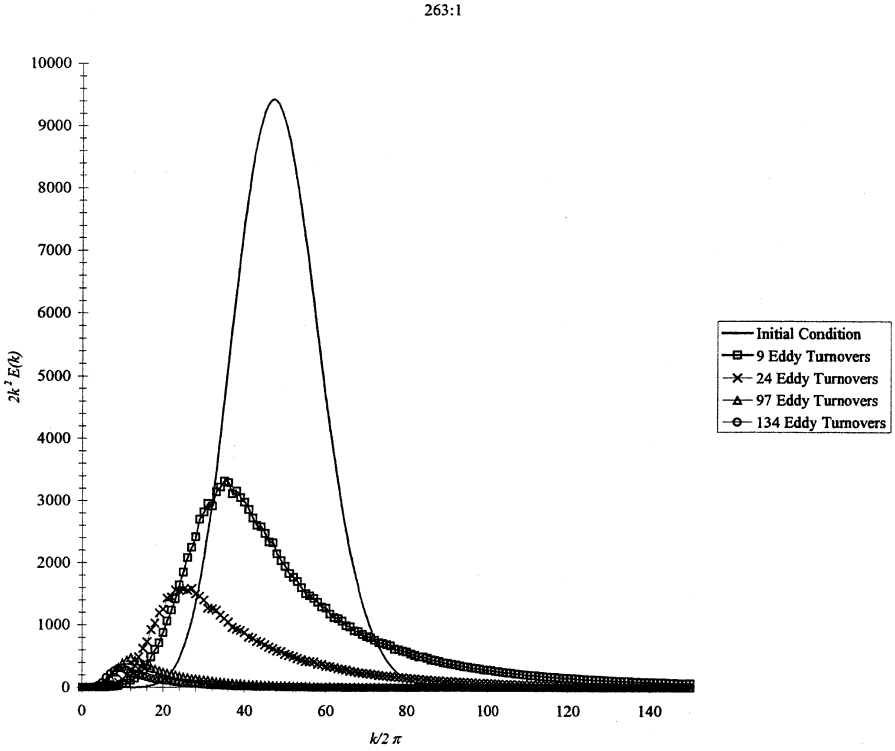

Fig. 9. The linear-linear plot of ensemble averaged enstrophy spectrum, $k^2E(k)$, plotted against wave number, $k/2\pi$, for $t = 0, 9, 24, 97$ and 134 eddy turnovers. Group B simulation.

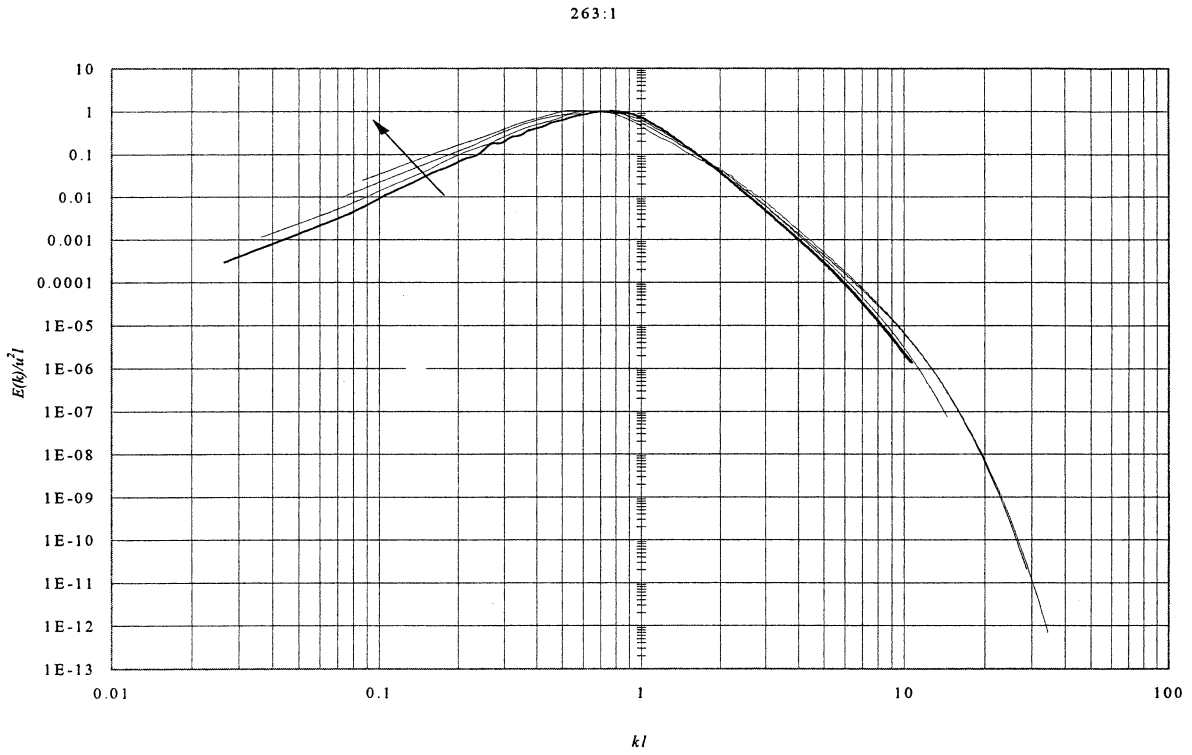

Fig. 10. The log-log plot of ensemble averaged normalised energy spectrum, $E(k)/u^2 l$, plotted against scaled wave number, kl, at 9, 24, 97 and 134 eddy turnovers (t/τ_e). Group B simulations. The arrow indicates increasing time.

Finally, in Fig. 11, we show the isocontours of vorticity for a run in which $\mathrm{Re} = 100$ and the box ratio is 100. The snapshots of the flow correspond to $t/t_e = 36, 96$, and 180. Two sets of pictures are shown corresponding to high and modest thresholds in the vorticity level. On the left the vorticity threshold corresponds to $\pm 2.5\omega_{\mathrm{rms}}$, where ω_{rms} is evaluated at $t/t_e = 36$. On the right the threshold is $\pm 0.75\omega_{\mathrm{rms}}$. It can be seen that a high threshold emphasises the coherent vortices, while the lower threshold allows the filamentary debris to be seen.

6. Discussion

We have shown that the integral-scale, l, grows approximately as $t^{1/2}$, in line with the simulations of [3] and [5]. Using l as a basis for a self-similar scaling, we find that the two-point vorticity correlations and energy spectrum collapse reasonably well onto a single, self-similar curve. However, this scaling does not capture the evolution of the low wave number, k^3, region of the energy spectrum, $E(k)$.

There is, as yet, no satisfactory explanation as to why the integral scale should grow as $t^{1/2}$. For low values of Re a $t^{1/2}$ growth in l would be expected, but $l \sim t^{1/2}$ is at odds with the various published theories of high-Re turbulence. A popular cartoon of high-Re turbulence, promoted by Bartello and Warn [6], is one in which the vorticity consists of a collection of intense, long-lived vortices immersed in a sea of weaker, filamentary vorticity. Existing theories can be viewed as variants of this cartoon, the various theories differing in the degree to which emphasis is placed on the coherent vorticity. For example, in Batchelor's original model the coherent vortices are completely ignored, and so we have filamentary vorticity acting on itself. In this case the integral scale grows because the vortex filaments are teased out into longer and longer strands, leading to the linear growth $l \sim t$. On the other hand, Carnevale et al. [22] adopted the reverse position, ignoring the filamentary vorticity and proposing a model in which the turbulence is dominated by coherent vortices. In their theory the integral scale grows as a result of vortex mergers, at a rate $l \sim t^{0.19}$. This is equally at odds with the numerical evidence.

There is, however, one simple physical process which leads to a non-diffusive growth of the form $l \sim t^{1/2}$. Although there is no direct evidence to suggest that it is *the* mechanism responsible for the observed $l \sim t^{1/2}$ it is, perhaps, worth a mention. This process involves an interaction between the coherent vortices (shown on the left of Fig. 11) and the background sea

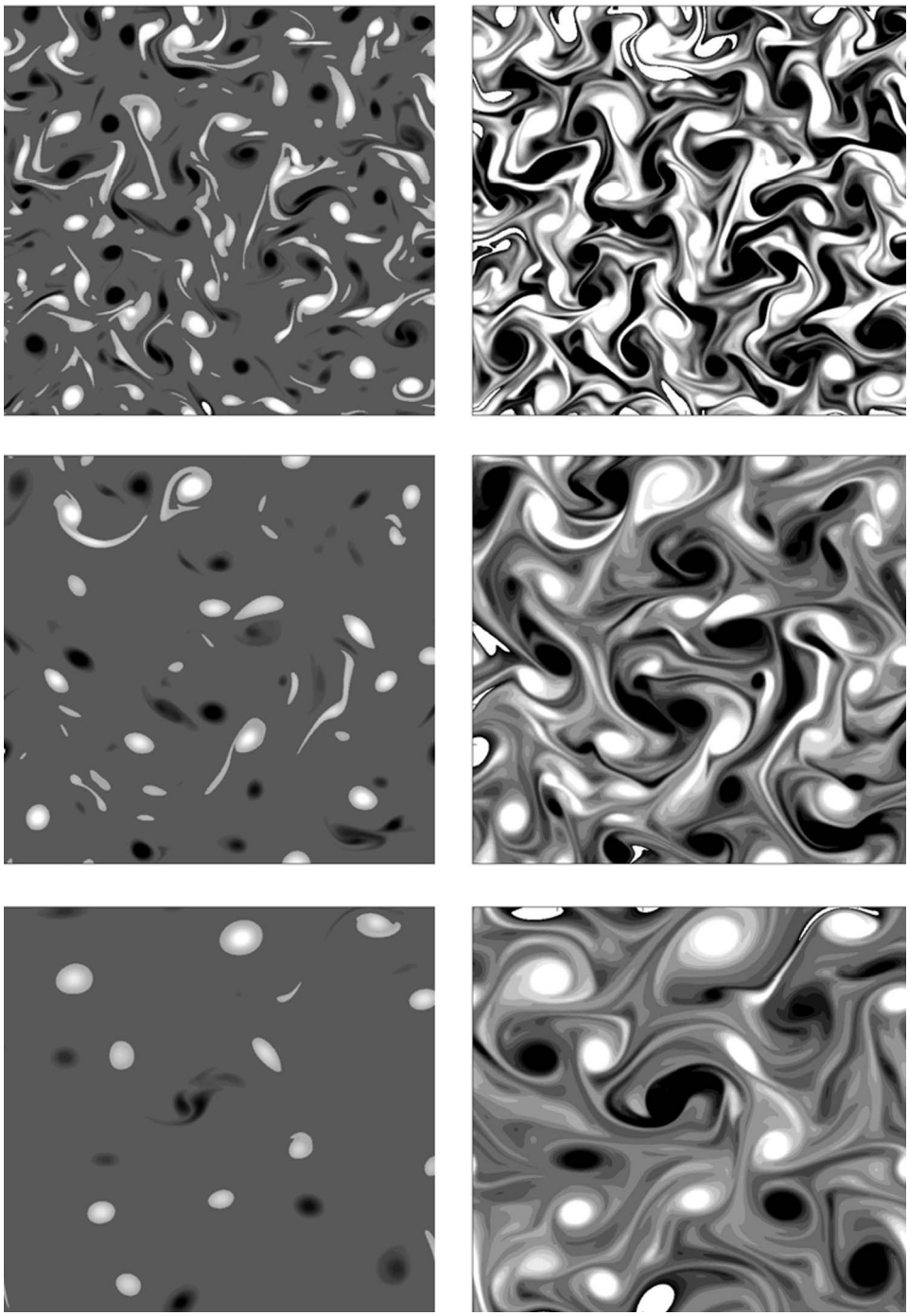

Fig. 11. Isocontours of vorticity for a run in which $\mathrm{Re} = 100$ and $B = 100$. The snapshots of the flow correspond to $t/t_e = 36, 96$, and 180. Two sets of pictures are shown corresponding to high and modest thresholds in the vorticity level. On the left the vorticity threshold corresponds to $\pm 2.5\omega_{\mathrm{rms}}$, where ω_{rms} is evaluated at $t/t_e = 36$. On the right the threshold is $\pm 0.75\omega_{\mathrm{rms}}$. The coherent vortices are evident on the left, while the filamentary debris can be seen on the right.

of filamentary debris (shown on the right of Fig. 11). In particular, coherent vortices can wind up the surrounding vorticity filaments, creating an eddy whose size grows as $t^{1/2}$. A simple model problem illustrates the idea.

Suppose that, at $t = 0$, we have a region of space where ω varies linearly with y, say $\omega = Sy$. (This represents the filamentary debris.) We now place a point vortex of strength Γ at the origin, which starts to wind up the vorticity field. For simplicity we assume that the velocity associated with $\omega(\mathbf{x}, t)$ is much weaker than that of the point vortex, so that $\mathbf{u} = (\Gamma/r)\hat{\mathbf{e}}_\theta$ in polar coordinates. Evidently ω evolves according to

$$\frac{\partial \omega}{\partial t} + \frac{\Gamma}{r^2}\frac{\partial \omega}{\partial \theta} = \upsilon \nabla^2 \omega \tag{20}$$

and it is readily confirmed that, if viscosity is neglected, the form of ω for $t > 0$ is,

$$\omega = Sr \sin[\theta - \Gamma t/r^2]. \tag{21}$$

This represents a progressive spiraling of the vorticity field by the point vortex. In fact, this solution is valid also for the viscous case, provided that r is much greater than the diffusive length-scale $\sqrt{\upsilon t}$ and $r^2/\Gamma t$ is greater than, or of the order of, unity. It is clear from the form of $\omega(r, \theta)$ in (21) that the integral scale of the eddy associated with the spiralled vorticity field grows as $l \sim \sqrt{\Gamma t}$.

It seems, therefore, that one possible explanation for the $t^{1/2}$ growth of the integral scale in two-dimensional turbulence involves the interaction of the coherent vorticity with the surrounding vortex filaments.

We conclude with a word of caution. Many numerical simulations of two-dimensional of turbulence use hyperviscosity to model dissipation, rather than a Newtonian model. It has been suggested that the way in which vortices and filaments interact in a hyperviscous fluid is different to that in a Newtonian fluid [9]. If this is the case, then there is the possibility that the $t^{1/2}$ scaling for l may not be observed in hyperviscous simulations and that consequently the enstrophy decay may differ from t^{-1}. The distinction between Newtonian and hyperviscous simulations remains an open issue.

Appendix A. A description of the DNS experiments

The *a priori* form of the initial energy spectrum used in the numerical simulations is,

$$E(k) = Qk^8 \exp\left(-4(k/k_p)^2\right), \tag{A.1}$$

where Q is a constant used to normalise the kinetic energy and k_p is the peak in the energy spectrum. Other initial conditions were tried and it was found that, while the initial development of the turbulence did depend on the form of $E(k)$ at $t = 0$, after twenty or so turnover times the initial conditions ceased to have much influence [18].

We use four groups (A, B, C and D) of ensemble averaged results in this paper. We also make use of the results from single realisation simulations (i.e. not ensemble averaged). The details of these individual simulations are described in the text where they appear. Table A.1, lists the specification of the ensemble averaged numerical experiments.

We estimate the isotropic vorticity correlations by sampling the correlation (for a fixed value of r) at the collocation points in physical space. To minimise the computational effort, we found it convenient to sample the correlation at distances defined by,

$$r_j = j\Delta x, \tag{A.2}$$

where Δx is the grid spacing and $j = 0, 1, \ldots, N/4$, i.e. we determine the vorticity correlation for a separation up to one quarter of the domain length. As noted by Lilly, [8], we can only determine $\omega\omega'(r)$ for a separation less than half of our computational

Table A.1
The specification of the two-dimensional turbulence DNS experiments

Description	Group A	Group B	Group C	Group D
Re	∼60	∼60	∼60	∼60
Box-ratio	540 : 1	263 : 1	131 : 1	100 : 1
Eddy turnover time ($\tau_e = l_0/u_0$)	0.00185	0.00380	0.00763	0.01
Number of realisations	16	48	48	48
Type of *a priori* spectrum	(A.1)	(A.1)	(A.1)	(A.1)
Number of modes	2048^2	1024^2	512^2	256^2

domain. This is because the periodic boundary conditions produce mirror image correlations with the axis of symmetry at $r = \frac{1}{2} l_{\text{dom}}$. We determine the spatially average value of $\omega\omega'$ using,

$$\overline{\omega\omega'(r_j)} = \frac{4}{N^2\omega^2}\left[\sum_{m=M/4}^{3M/4}\sum_{n=N/4}^{N/2}\omega(m,n)\omega(m,n+j) + \sum_{m=M/4}^{M/2}\sum_{n=N/4}^{3N/4}\omega(m,n)\omega(m+j,n)\right]. \tag{A.3}$$

Note that we sample in both the x and y directions.

References

[1] G.K. Batchelor, Computation of the energy spectrum in homogeneous two-dimensional turbulence, Phys. Fluids Suppl. II (1969) 233–239.
[2] J.R. Chasnov, On the decay of two-dimensional homogeneous turbulence, Phys. Fluids 9 (1) (1997).
[3] H.J.H. Clercx, A.N. Nielsen, Vortex statistics for turbulence in a container with rigid boundaries, Phys. Rev. Lett. 85 (4) (2000) 752–755.
[4] S. Ossia, M. Lesieur, Large-scale energy and pressure dynamics in decaying two-dimensional incompressible isotropic turbulence, J. Turbulence 2 (2001) 013.
[5] J.R. Herring, Y. Kimura, J. Chasnov, Evolution of Decaying Two-dimensional Turbulence and Self-similarity, Trends in Mathematics, Birkhäuser Verlag Basel, Switzerland, 1999.
[6] P. Bartello, T. Warn, Self-similarity of decaying two-dimensional turbulence, J. Fluid Mech. 326 (1996) 357–372.
[7] J.C. McWilliams, The emergence of isolated coherent vortices in turbulent flow, J. Fluid Mech. 146 (1984) 21–43.
[8] B. Legras, D.G. Dritschel, P. Caillol, The erosion of a distributed two-dimensional vortex in a background straining flow, J. Fluid Mech. 441 (2001) 369–398.
[9] A. Mariotti, A. Legras, D.G. Dritschel, Vortex stripping and the erosion of coherent structures in two-dimensional flows, Phys. Fluids 6 (12) (1994) 3954–3962.
[10] D.K. Lilly, Numerical simulation of developing and decaying two-dimensional turbulence, J. Fluid Mech. 45 (2) (1971) 395–415.
[11] P.A. Davidson, Turbulence: An Introduction for Scientists and Engineers, Oxford University Press, 2004.
[12] R.H. Kraichnan, Inertial ranges in two-dimensional turbulence, Phys. Fluids 10 (1967) 1417–1423.
[13] A.N. Kolmogorov, The local structure of turbulence in incompressible viscous fluid for very large Reynolds number, Proc. R. Soc. London Ser. A 434 (1991) 9–13.
[14] R.H. Kraichnan, D. Montgomery, Reports on Progress in Physics 43 (2) (1980) 549–619.
[15] G.K. Batchelor, The Theory of Homogeneous Turbulence, Cambridge University Press, 1953.
[16] S.A. Orszag, G.S. Patterson, Numerical simulation of three-dimensional homogeneous isotropic turbulence, Phys. Rev. Lett. 28 (1972) 76–79.
[17] D.G. Fox, S.A. Orszag, Pseudospectral approximation to two-dimensional turbulence, J. Comput. Phys. 11 (1973) 612–619.
[18] A.J. Lowe, The direct numerical simulation of isotropic two-dimensional turbulence in a periodic square, Cambridge University Engineering Dept. Thesis, 2001.
[19] C. Canuto, M.Y. Hussaini, A. Quarteroni, T.A. Zang, Spectral Methods in Fluid Mechanics, Springer-Verlag, 1988.
[20] R.S. Rogallo, Numerical experiments in homogeneous turbulence, Report No. NASA TM-81315, AMES Research Centre, NASA, 1981.
[21] J.R. Herring, S.A. Orszag, R.H. Kraichnan, D.G. Fox, Decay of two-dimensional homogeneous turbulence, J. Fluid Mech. 46 (3) (1974) 417–444.
[22] G.F. Carnevale, J.C. McWilliams, Y. Pomeau, J.B. Weiss, W.R. Young, Evolution of vortex statistics in two-dimensional turbulence, Phys. Rev. Lett. 66 (1991) 2735–2737.